Journal of Renewable Energy and Sustainable Development (RESD) Volume 11, Issue 1, June 2025 - ISSN 2356-8569
http://dx.doi.org/10.21622/RESD.2025.11.1.1223

Received on, 10 February 2025 Accepted on, 25 March 2025 Published on, 10 April 2025

Impact of Ammonia-water Concentrations on Solar Absorption Refrigeration Performance

Mohammed El Amine Chikh *[1], Mohammed Benramdane [2], Abdennour Aliane [3], and Bilal Abdesselam [4]

[1,2,3,4] An Applied Energy and Thermal Laboratory (ETAP), Department of Mechanical Engineering, Faculty of Technology, Abou Bekr Belkaid University, Tlemcen, Algeria

mohammedelamine.chikh@univ-tlemcen.dz, benramdane2006@yahoo.fr, abdennouraliane@yahoo.fr, bilalalbert24@gmail.com

ABSTRACT

Increased demand for summer comfort due to heat waves is driving the adoption of absorption refrigeration systems. These systems use free solar energy and environmentally friendly refrigerants, offering a sustainable solution despite their lower efficiency. This study investigates the effect of refrigerant ammoniac (NH_3) mass concentration on the performance parameters of a single-effect solar absorption refrigeration system using the NH3/H2O binary pair. A thermodynamic model is developed to evaluate the system's coefficient of performance (COP) under varying generator temperatures, evaporator temperatures, and pressures. Results show that the COP increases significantly with NH_3 concentrations up to a threshold (23-25%), beyond which it stabilizes. Optimal performance is achieved at a generator temperature of 114°C, a low pressure of 1 bar, and an NH_3 concentration of 25%, yielding a maximum COP of 1.29. Additionally, the COP decreases with higher evaporator temperatures and pressures, highlighting the critical influence of thermodynamic parameters. This analysis underscores the importance of optimizing NH_3 concentrations and system operating conditions to maximize energy efficiency and facilitate sustainable cooling applications in solar-rich regions.

Index-words: *Refrigeration, Absorption, COP, Solar energy, NH_3-H_2O.*

Nomenclature	
COP	coefficient of performance [-]
P	pressure [bar]
Ex	heat exchanger efficiency [-]
h	enthalpy [kJ/kg]
$\dot{m}$	mass flow rate [kg/s]
Q	heat transfer rate in system component [KW]
T	temperature [°C]
W	pump work [KW]
x	mass concentration [%]
Subscripts	
a	absorber
c	condenser
ev	evaporator
g	generator
h	high
b	low
m	ambient
In	inlet condition
out	outlet condition
Abbreviations	
H_2O	water
LiBr	lithium bromide
NH_3	ammoniac
VARS	*vapor absorption refrigeration system*

Copyright © 2025, authors

Volume 11, Issue 1, June 2025 - ISSN 2356-8569
http://dx.doi.org/10.21622/RESD.2025.11.1.1223

I. INTRODUCTION

The manuscript Renewable energy is rapidly growing worldwide due to environmental and geopolitical concerns [1]. According to the International Energy Agency [2] [3], air conditioning is the fastest-growing energy consumption sector in buildings. Energy consumption for air conditioning is expected to more than double in the next 30 years, leading to increased electricity consumption peaks, especially in hot countries [4], [5], [6]. Sorption chillers use heat sources such as solar energy, thus reducing electricity consumption for cooling. These systems can operate continuously (absorption) or in alternating cycles (adsorption). Their performance depends on the choice of working pairs and the design of sorption elements. Recent developments have improved the efficiency and capacity of heat exchangers in absorption machines, while adsorption chillers require specific exchangers [7], [8].

The most common working pairs used in absorption systems are H_2O-LiBr and NH_3-H_2O. However, each has drawbacks that limit the application and development of absorption chillers [9], [10]

Several researchers have studied the implementation of vapor absorption refrigeration systems (VARS) using H_2O-LiBr as the working pair. This binary pair is commonly used for air conditioning applications, as it can maintain an evaporation temperature down to 5°C. For temperatures below 5°C, the NH_3-H_2O pair is effectively employed in VARS [11].

Sieres and Fernández-Seara [12] conducted a study on the impact of the component dimensions of the distillation column on vapor enrichment and the performance of small-scale NH_3–H_2O absorption refrigeration systems. The results demonstrate an improvement in system efficiency, with a COP value of 0.55 achieved through an optimized configuration of the stripping section and rectifier. This design minimizes water accumulation in the evaporator while maximizing the overall system performance.

Kumar et al. [13] analyze a single-effect LiBr-H_2O absorption system using waste heat from steam turbines in the sugar industry. The results show that the COP varies as a function of operating parameters: it decreases with an increase in cooling water inlet temperature (25-30°C) and circulation ratio but can reach optimum values for specific conditions. For example, for a concentration of 50% weak solution, the COP varies from 0.4 to 0.6. The study highlights energy efficiency and potential savings in an industrial context.

Hılali and Söylemez [14] propose an engine exhaust gas-driven absorption cooling system for automobile air-conditioning. Compared to the conventional vapor compression system, this system achieves a cooling capacity ranging from 0.5 kW at idle to 2.8 kW under full load. The system's coefficient of performance (COP) is around 0.18. The recovered heat from the exhaust gases ranges from 3 kW to 16 kW, improving the cooling efficiency and reducing fuel consumption due to lower back pressure.

Marcos et al. [15] propose a double-effect LiBr air/water absorption solar cooling system designed for hot and arid climates. Compared to the conventional single-effect water-cooled system, this system reduces water consumption by 35,377 m^3/year, saves 1,253 MWh of energy, and cuts CO_2 emissions by 11,008 tons/year. It also offers superior efficiency with a COP improvement of 19–48%.

Yıldırım and Yeşilata [16] optimized a Li-Br/water absorption system using a low-temperature heat source with the Structural Bond Coefficients method. The optimization reduced system irreversibility by 72.5%, though it increased initial costs. However, the additional investment is recovered in 4.2 years. The study highlights the potential of integrating solar thermal collectors to enhance efficiency. Given the rising cost of conventional energy, the payback period may be shortened in the future. The research emphasizes the balance between thermodynamic performance and economic feasibility.

Ramesh et al. [17] investigated a shell and helical coil solution heat exchanger in an NH_3-H_2O vapor absorption refrigeration system. The solution heat exchanger achieved effectiveness of 0.84–0.9. The system's COP improved by up to 60% with solution heat exchanger integration, highlighting its potential for enhanced heat recovery and efficiency.

Wang et al. [18] studied an absorption refrigeration system based on NH_3-H_2O-LiBr by developing an accurate thermodynamic model (vapor-liquid equilibrium) validated by experimental data (error <9.6%). The simulations show that the addition of LiBr improves the COP (with a deviation <0.02) by reducing distillation losses but requires an optimum

Volume 11, Issue 1, June 2025 - ISSN 2356-8569
http://dx.doi.org/10.21622/RESD.2025.11.1.1223

concentration to avoid absorption problems. The model can be used to optimize temperatures and concentrations for maximum performance.

Kilic and Ipek [19] have studied a solar absorption cooling system using the nanofluid LiBr-Al_2O_3-H_2O as the working fluid. The nanoparticles increase thermal conductivity and heat transfer, thereby improving system performance. Increasing the concentration of Al_2O_3 (0% to 0.1%) and the temperature of the generator (75°C to 85°C) resulted in an increase in the COP, reaching a maximum of 0.86. However, increased viscosity can lead to pressure losses, requiring a balance between thermal conductivity and viscosity.

Kumar et al. [20] optimized an NH_3-H_2O absorption refrigeration system using energy and exergy analyses. The optimal generator temperature for maximum COP (0.54) is 99 °C, while for minimum exergy destruction, it is 88 °C, 11 °C lower. Increasing the evaporator temperature reduces the required cut-off temperature, while a higher condenser temperature increases it. The results highlight the effectiveness of the exergy-based approach for optimizing such systems.

From the literature reviewed, there has been much on studying the effect of ammonia as a refrigerant fluid. It has been found that significant improvements can be made to the technical aspects of solar absorption cooling systems.

Despite the benefits that ammonia provides to absorption refrigeration systems, its excessive use presents several challenges: it is expensive, toxic, not environmentally friendly, and difficult to obtain.

As a result, this study focuses on proposing a thermodynamic model to evaluate the performance of a single-effect solar absorption cooling system. This system is simple, easy to install, compact, portable, and easy to maintain. Most importantly, it operates using solar energy instead of non-renewable energy sources.

However, a high cooling capacity and a coefficient of performance (COP) of 1.29, along with an absorption cooling temperature reaching -30 °C, can be achieved through this theoretical analysis of the influence of various parameters, followed by validation with previous studies. This is particularly beneficial for industries such as cold storage for food, medicine, and industrial tools.

The primary modification introduced in this system is the reduction of ammonia concentration (X_{NH_3}) in the refrigerant solution. As mentioned earlier, ammonia is a laboratory-produced substance that is toxic and, therefore, not environmentally friendly. So reducing it is better. This adjustment aims to enhance the coefficient of performance (COP) while reducing pollutant emissions, all without compromising the system's optimal thermodynamic efficiency.

By carefully optimizing the operating conditions and adjusting key system parameters, we ensured that the system's energy efficiency matched or surpassed the performance of existing systems. These efforts represent a significant contribution to the advancement of environmentally friendly and energy-efficient refrigeration technologies.

II. SOLAR REFRIGERATION

Sorption chillers use heat sources, such as solar energy, to drive the cooling process, significantly reducing electricity consumption compared to conventional cooling systems.

A typical thermo-solar cooling system (Figure 1) consists of an absorption chiller integrated

with a solar thermal energy source. This configuration harnesses solar radiation to generate the necessary thermal energy, which is then used to power the absorption cycle, producing the desired cooling effect. The system contributes to energy efficiency and sustainability by reducing dependence on conventional electricity-driven refrigeration technologies.[3]

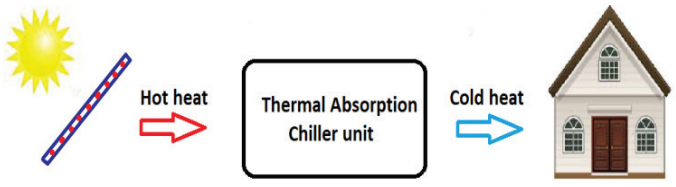


Fig. 1. General diagram of a thermo-solar cold production system

Absorption systems exhibit a wide range of configurations, each tailored to specific operational requirements and energy sources. They can be classified based on their heat input method, such as direct combustion, solar energy, or waste heat recovery. The cycle complexity also varies, with single-effect, double-effect, and multi-effect systems

Volume 11, Issue 1, June 2025 - ISSN 2356-8569
http://dx.doi.org/10.21622/RESD.2025.11.1.1223

designed to optimize energy efficiency. The choice of the working fluid, commonly NH_3/H_2O or $LiBr/H_2O$, influences the system's applicability and operating conditions. Additionally, these systems differ in their cooling mechanisms, utilizing either air-cooled or water-cooled heat sinks. Their applications range from small-scale residential cooling to large industrial refrigeration, with systems designed for either continuous operation, ensuring stable cooling or discontinuous cycles suited for intermittent energy sources. [21]

A. *Absorption Refrigeration*

The single-effect solar absorption refrigeration system has been selected using the NH_3/H_2O binary mixture. This cycle operates at two pressure levels (high and low), as illustrated in Figure 2.

In a solar absorption refrigeration system using the NH_3/H_2O pair, the cycle begins in the generator, where the liquid solution is heated by solar energy collected through solar panels (Qg), causing the separation of the refrigerant (NH_3) from the absorbent (H_2O). The ammonia vapor produced is then directed to the condenser, where it releases heat to the environment (Qc) and condenses into a liquid. This liquefied refrigerant passes through an expansion valve, which lowers its pressure and temperature via the Joule-Thomson effect, facilitating its evaporation in the evaporator, where it absorbs the thermal load (Qev) from the surrounding medium. The resulting NH_3 vapor is then sent to the absorber, where it dissolves in the water solution, a process that releases heat (Qa) to an external cooling fluid. The NH_3/H_2O solution, now at low temperature and pressure, is pumped back to the generator through a heat exchanger, which helps recover part of the thermal energy from the fluid leaving the generator, improving the system's overall efficiency. The absorbent (H_2O), at high temperature and pressure, also flows from the generator to the absorber through a heat exchanger and an expansion valve. This cycle repeats continuously, ensuring efficient cooling while utilizing solar energy as the primary power source. [22], [23]

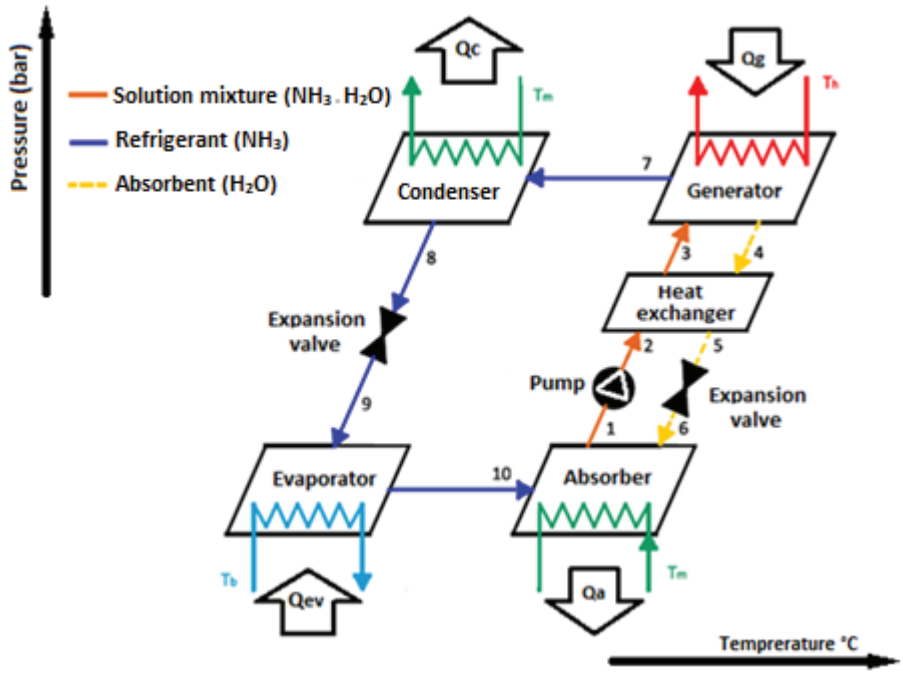


Fig. 2. Basic diagram of a solar absorption refrigeration machine single-effect

B. *Thermal Storage*

The single-effect absorption cycle represents the fundamental configuration of solar absorption cooling technologies. It typically consists of three essential components: the solar collector, the energy storage system, and the absorption machine [24] (Figure 3).

http://dx.doi.org/10.21622/RESD.2025.11.1.1223

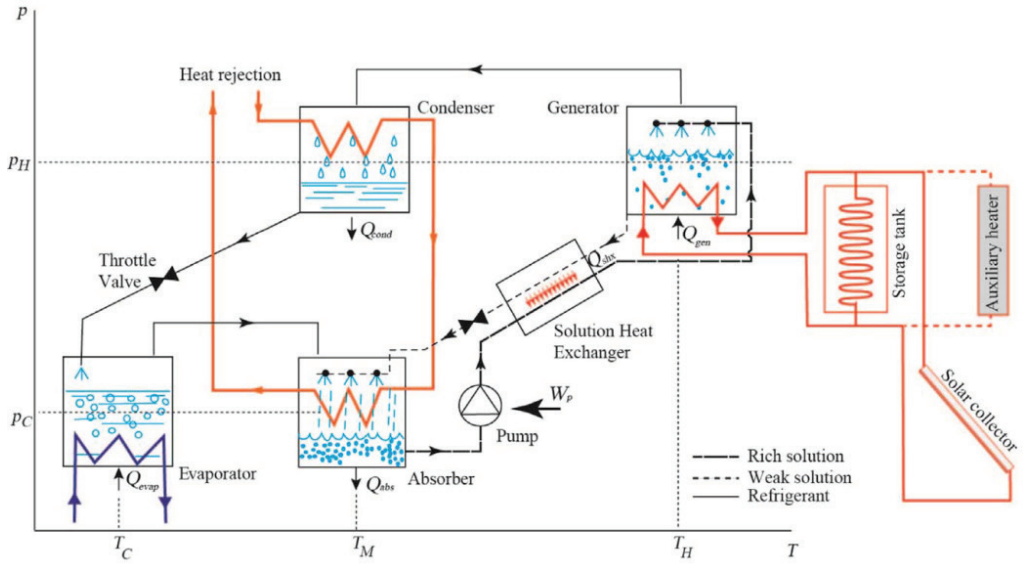


Fig. 3. Schematic of a single-effect solar absorption chiller with storage unit and solar collector [25]

The thermal energy required to operate these technologies comes from sunlight. The solar thermal system converts solar radiation through the greenhouse effect and absorption by the collector. This process is known as solar irradiation[26] [27]. This thermal energy then feeds the system, specifically the generator.

The working heat supplied by the conventional heater is partially replaced by solar heat. When heat production exceeds requirements, the surplus is stored in the storage tank for later use. If there is insufficient sunshine or at night, an auxiliary heater takes over [28].

Currently, most solar cooling systems available on the market operate according to this principle, using flat-plate or evacuated-tube solar collectors to supply the heat [29]. Thermal storage helps mitigate the intermittency of solar systems by extending their operating time and improving efficiency. There are three main types of storage: sensible heat storage, which offers high efficiency but requires temperature variations; latent heat storage, which allows constant temperature storage but still requires further research; and thermochemical cycle storage, which remains experimental. Heat transfer fluid storage tanks are commonly used, though their performance is affected by heat losses due to fluid mixing. [30]

III. THERMODYNAMIC STUDY

The thermodynamic modeling carried out for the different refrigeration cycles is based on the first law of thermodynamics [31], [32], [33]. The general form of the mass and energy conservation equations is as follows:

$$\sum \dot{m}_{in} = \sum \dot{m}_{out} \quad (1)$$

$$\sum \dot{m}_{in}\, x_{in} = \sum \dot{m}_{out}\, x_{out} \quad (2)$$

$$\sum Q + \sum W = \sum \dot{m}_{out} h_{out} - \sum \dot{m}_{in} h_{in} \quad (3)$$

The detailed equations for the single-effect cycle case are as follows:

A. Mass Balance

Generator

$$\dot{m}_3 = \dot{m}_4 + \dot{m}_7 \quad (4)$$

$$x_3 = x_r \quad (5)$$

$$x_4 = x_p \quad (6)$$

$$x_3 \dot{m}_3 = x_4 \dot{m}_4 \quad (7)$$

Condenser

$$\dot{m}_7 = \dot{m}_8 \quad (8)$$

Evaporator

$$\dot{m}_9 = \dot{m}_{10} \quad (9)$$

http://dx.doi.org/10.21622/RESD.2025.11.1.1223

Absorber

$$x_1\dot{m}_1 = x_6\dot{m}_6 \quad (10)$$

$$\dot{m}_6 + \dot{m}_{10} = \dot{m}_1 \quad (11)$$

Heat exchanger

$$\dot{m}_3 = \dot{m}_2 \quad (12)$$

$$\dot{m}_5 = \dot{m}_4 \quad (13)$$

Expansion valve

$$\dot{m}_8 = \dot{m}_9 \quad (14)$$

$$\dot{m}_5 = \dot{m}_6 \quad (15)$$

B. Energy balance

Generator

$$Q_g = \dot{m}_4\, h_4 + \dot{m}_7\, h_7 - \dot{m}_3\, h_3 \quad (16)$$

Condenser

$$Q_c = \dot{m}_7\, h_7 - \dot{m}_8\, h_8 \quad (17)$$

Evaporator

$$Q_{ev} = \dot{m}_{10}\, h_{10} - \dot{m}_9\, h_9 \quad (18)$$

Absorber

$$Q_a = \dot{m}_{10}\, h_{10} + \dot{m}_6\, h_6 - \dot{m}_1\, h_1 \quad (19)$$

Heat exchanger

$$Q_{ex} = \dot{m}_3\, h_3 - \dot{m}_2\, h_2 \quad (20)$$

$$Q_{ex} = \dot{m}_4\, h_4 - \dot{m}_5\, h_5 \quad (21)$$

Expansion valve

$$Q_{8-9} = \dot{m}_9\, h_9 - \dot{m}_8\, h_8 \quad (22)$$

$$Q_{5-6} = \dot{m}_6\, h_6 - \dot{m}_5\, h_5 \quad (23)$$

Pump

The circulation pump transports the refrigerant-rich solution to the high-pressure generator:

$$W = \dot{m}_1\ (h_6 - h_5) \quad (24)$$

Coefficient of performance

The coefficient of performance (**COP**) of the absorption refrigeration system is defined as:

$$COP = \frac{Q_{ev}}{Q_g + W} \quad (25)$$

The determination of the various thermodynamic parameters is based on the use of the Oldham (Figure 4) and Merkel (Figure 5) diagrams.**[5] [34], [35]**

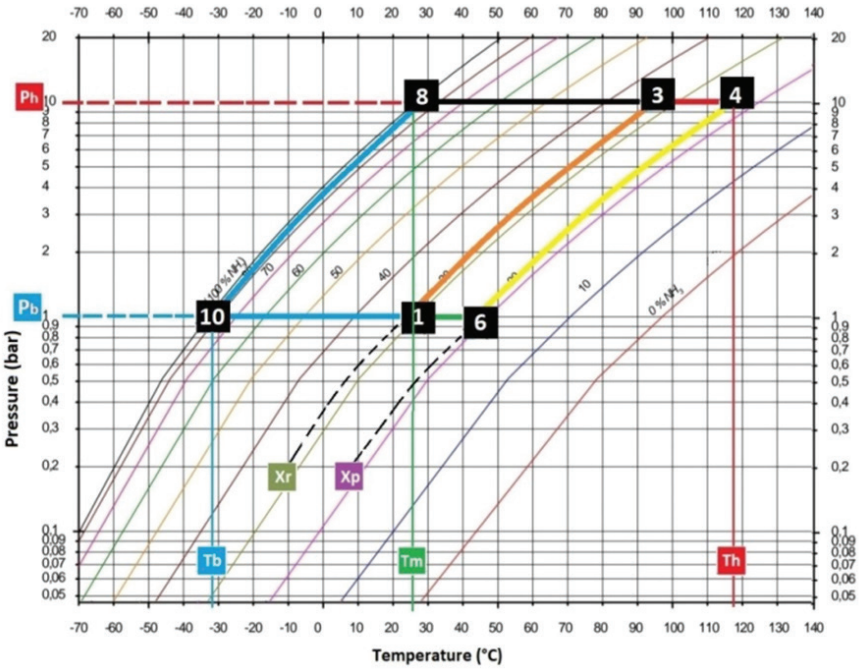


Fig. 4. Representation of the absorption cycle on the diagram of Oldham for NH3/H2O, (P, T)

Volume 11, Issue 1, June 2025 - ISSN 2356-8569
http://dx.doi.org/10.21622/RESD.2025.11.1.1223

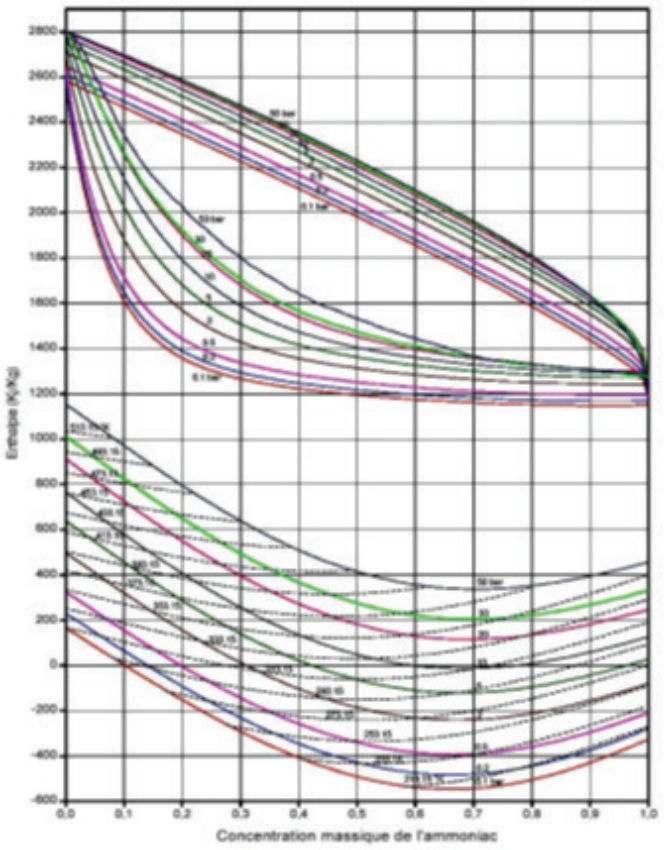


Fig. 5. Automated Merkel diagram

IV. WORKING CONSTRAINTS

A. Hypotheses

In order to obtain a match between the chosen model and the considered unit, certain assumptions have been imposed. We consider that there are no heat losses to the outside environment.

- The expansion is isenthalpic at the valve level.
- Variations in kinetic energy and potential energy are negligible.
- The system is adiabatic, without heat losses. (necessary to develop a thermodynamic model that isolates key performance parameters).
- Steady-State Operation (the system operates dynamically with fluctuating solar radiation and ambient conditions for a more precise evaluation).

B. Input Parameters

Taking into account the reference data [36], the studied installation operates according to the single-effect absorption cycle using the binary pair (NH_3-H_2O) ammonia-water (NH_3 as refrigerant fluid and H_2O as absorbent fluid) Figure 2, with the following operating conditions:

- $1 \leq Pb \leq 1.7$ bar: low pressure.
- Ph = 7 bar: high pressure.
- Tm = 25°C : Ambient temperature
- Ex = 0.83: heat exchanger efficiency
- $\dot{m}_1 = 1$ [kg/s]: Rich solution mass flow rate (NH_3/H_2O)
- $\dot{m}_7 = 0.45$ [kg/s]: Refrigerant mass flow rate (NH_3)
- x_r = 33%: mass concentration of the mixture (NH_3/H_2O) at point 1 (rich solution)
- 14% ≤ x_{NH_3} ≤ 25%: NH_3 mass concentration at point 4.

V. MODEL SETUP

Developing a mathematical model for a Single-Effect Solar Absorption system is essential for gaining a deeper understanding of its operational behavior, optimizing its performance, and minimizing development time, construction costs, and associated risks.

Several studies have employed different simulation tools to model cooling systems, such as TRNSYS [37], MATLAB [38], and TRANSOL [39], [40]. In this study, the Engineering Equation Solver (EES) software was selected due to its strong relevance to thermodynamic applications and its ability to efficiently handle complex equations related to energy systems [41], [42] .

EES provides a robust platform for designing and analyzing heat and cooling system models within the thermal liquid domain. It allows for the consideration of key thermodynamic properties such as temperature variations, viscosity changes, and heat transfer effects. These variations result from both internal processes within the system components and external influences from environmental conditions. By using EES, it becomes possible to accurately simulate the performance of the absorption system, assess its efficiency, and explore potential improvements.

Volume 11, Issue 1, June 2025 - ISSN 2356-8569
http://dx.doi.org/10.21622/RESD.2025.11.1.1223

VI. WORKING FLUID

The key advantages of NH_3 over H_2O as a refrigerant include its significantly lower freezing point, making it suitable for subzero cooling applications. Its higher working pressures allow the system to achieve negative cooling temperatures without requiring deep vacuum conditions, which simplifies system design. Unlike H_2O, which operates under vacuum in absorption cycles, NH_3 can function at moderate pressures, reducing the need for expensive and specialized vacuum components [9]. Additionally, NH_3 has a high latent heat of vaporization, enhancing its cooling capacity while maintaining efficiency. Its compatibility with metallic components also contributes to system durability and reliability.[21], [43], [44]

VII. RESULTS AND DISCUSSION

The different results presented in this work are obtained from the resolution of the equations of the developed model above, using the EES software to solve these equations.

To operate an NH_3/H_2O absorption machine efficiently, it is crucial to correctly select the concentrations of the binary pair as well as the temperatures and pressures at the generator, evaporator and absorber levels.

A. Model Validation

The results of our models are compared with COP values reported in previous studies to validate their accuracy and performance.

Al-Rbaihat et al. [45] achieved a maximum COP of 0.8483 under optimal operating conditions. These conditions included a generator pressure of Ph = 14.5 bar, an evaporator pressure of Pb = 2.8 bar, a generator temperature of Tg = 135°C, and an evaporator temperature of Te = -6°C. This highlights the importance of precise pressure and temperature control in maximizing system efficiency.

Similarly, Khan et al. [46] reported a COP of 0.8, derived based on the first law of thermodynamics. Their optimal conditions involved a generator temperature of Tg = 120°C and an evaporator temperature of Te = -2.2°C.

Wei Wu et al. [47] presented an experimental study on a Compression-Assisted Absorption Heat Pump using an ammonia-water binary mixture to improve efficiency. The tests showed that when the generator temperature reached 115°C, the attained COP was 1.271, with the evaporator temperature at -10°C.

These studies emphasize the role of temperature ranges and operating conditions in determining the thermodynamic efficiency of refrigeration systems, offering a useful benchmark for comparison with our model's results.

B. Interpretations

The following figures show the effect of generator temperature (Tg) and evaporator temperature (Tev) on the coefficient of performance (COP) with different in low pressure (Pb) and the different various ammonia concentrations (X_{NH_3}), ranging from 14% to 25%.

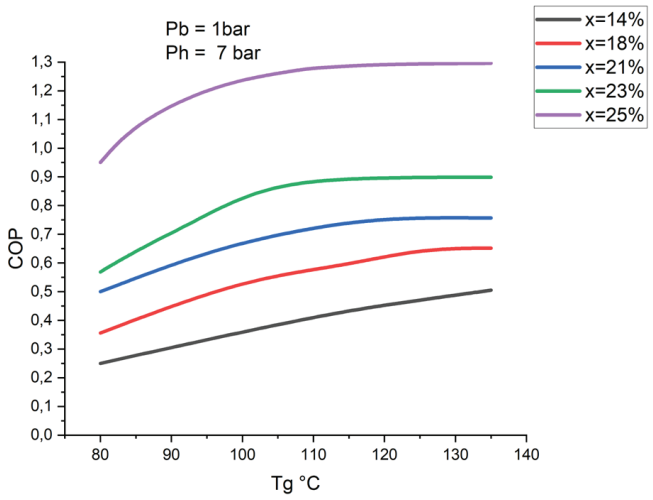


Fig. 6. Variation of the coefficients of performance with generator temperature (Tg) for Pb=1bar

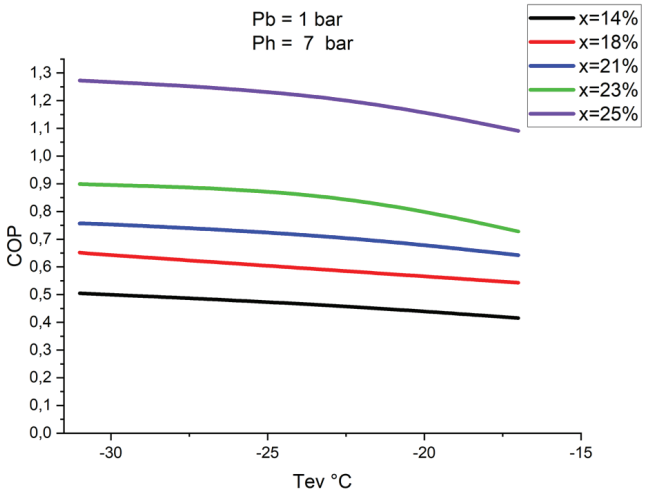


Fig. 7. Variation of the coefficients of performance with evaporator temperature (Tev) for Pb=1bar

Volume 11, Issue 1, June 2025 - ISSN 2356-8569
http://dx.doi.org/10.21622/RESD.2025.11.1.1223

In Figure 6. For Pb = 1 bar, when the ammonia concentration X_{NH_3} is low, i.e., 14%, 18%, or 21%, the COP increases proportionally to the generator temperature Tg = 135°C, the corresponding COPs are 0.505, 0.652, and 0.7565 respectively. By increasing the concentration in X_{NH_3}, two distinct phases are observed. In the first, the generator temperature increases proportionally to the COP, regardless of the value of X_{NH_3}. In the second, after a certain temperature threshold, the COP stabilizes and becomes almost constant beyond Tg = 109°C, reaching a value of 0.8984 for X_{NH_3} = 23% and 1.285 for X_{NH_3} = 25% at Tg = 114°C.

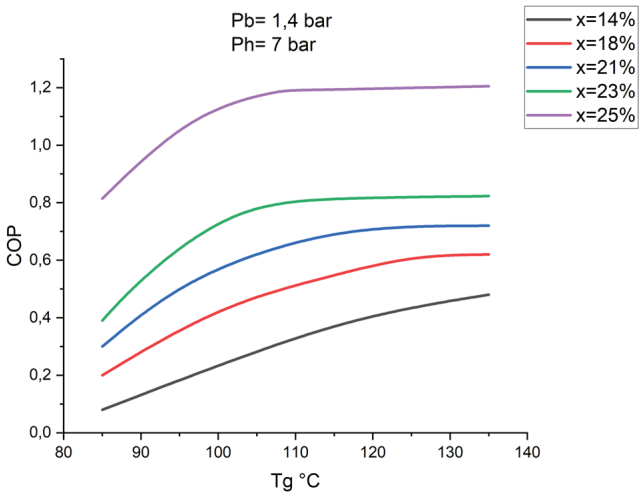


Fig. 8. Variation of the coefficients of performance with generator temperature (Tg) for Pb=1.4 bar

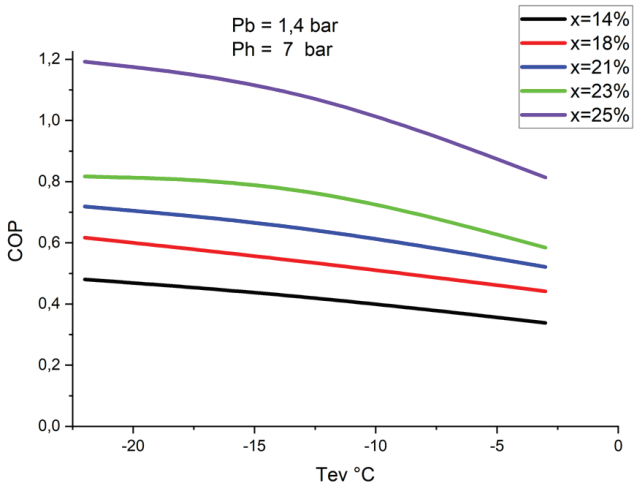


Fig. 9. Variation of the coefficients of performance with evaporator temperature (Tev) for Pb=1.4 bar

The Figure 8. For Pb = 1.4 bar, the generator temperature is proportional to the COP when the ammonia concentration X_{NH_3} is low, namely 14%, 18%, and 21%, with a COP value of 0.480, 0.620, and 0.720 respectively, at a generator temperature Tg = 135°C. By increasing the concentration in X_{NH_3}, two distinct behaviors appear. In the first range, an increase in temperature with a proportional increase in COP, regardless of the value of X_{NH_3}. In the second range, from a certain generator temperature, the COP stabilizes and remains almost constant after Tg = 117°C, reaching a value of 0.817 for X_{NH_3} = 23% and 1.192 for X_{NH_3} = 25% at Tg = 108°C.

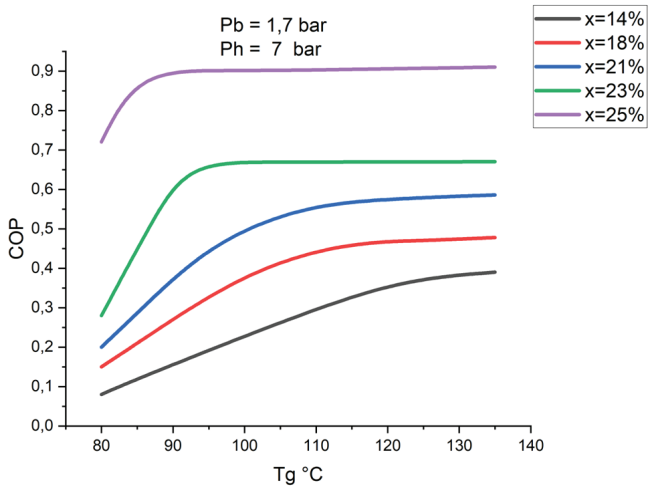


Fig. 10. Variation of the coefficients of performance with generator temperature (Tg) for Pb=1.7 bar

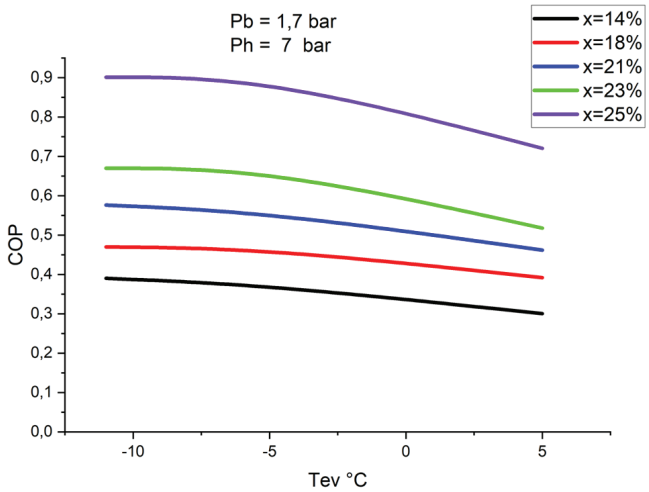


Fig.11. Variation of the coefficients of performance with evaporator temperature (Tev) for Pb=1.7 bar

In Figure 10. For Pb = 1.7 bar, the generator temperature is proportional to the COP for low concentration X_{NH_3} = 14% at a value of 0.39, X_{NH_3} = 18% at a value of 0.478, and X_{NH_3} = 21% at a value of 0.586 in Tg = 135°C. By increasing the concentration of X_{NH_3}, it is noted that there are two ranges: the

Volume 11, Issue 1, June 2025 - ISSN 2356-8569
http://dx.doi.org/10.21622/RESD.2025.11.1.1223

first range varies, and increasing the temperature is proportional to the COP for any choice of the value of X_{NH_3}. In the second range, at a certain generator temperature, the COP curve becomes constant starting from Tg = 92 °C at a value of 0.668 for X_{NH_3} = 23% and 0.9002 starting from Tg = 85°C for X_{NH_3} = 25%.

For Figure 7, Figure 9, and Figure 11, it is observed that the COP variation is inversely proportional to the evaporator temperature (Tev): the COP decreases as the evaporator temperature increases within the same temperature range, regardless of the variation in concentrations X_{NH_3}. Additionally, it is noted that the COP decreases with increasing pressure (Pb).

Table I represents the good choice of thermodynamic parameters for better operation at the generator level of the absorption installation (concentration, temperature, and pressure), which is a very important element.

TABLE I. MAXIMUM COP VALUES FOR DIFFERENT PRESSURES AND CONCENTRATIONS

X_{NH_3}		14%	18%	21%	23%	25%
COP	Pb=1	0.505	0.652	0.7565	0.899	1.296
	Pb=1.4	0.4805	0.620	0.720	0.823	1.205
	Pb=1.7	0.390	0.478	0.586	0.6702	0.910

These studies underscore the impact of temperature and operating conditions on refrigeration efficiency, serving as a benchmark for our model.

VIII. CONCLUSION

The objective of this contribution is to highlight the solar absorption refrigeration system.

The in-depth analysis of the effect of the ammonia (NH_3) mass concentration on the performance of the single-effect solar absorption refrigeration system (using the NH_3-H_2O binary pair) has revealed several key trends. The results clearly show that the NH_3 concentration directly affects the coefficient of performance (COP) (a crucial indicator of system efficiency).

When the ammonia mass concentration (X_{NH_3}) is relatively low (between 14% and 21%), an increase in the generator temperature leads to a significant improvement in the COP. For example, for a concentration of 21%, the COP reaches 0.7565 at a generator temperature of 135°C, keeping the low pressure constant and equal to one (01) bar. However, this correlation is not proportional to high X_{NH_3}. Indeed, for concentrations of 23% and 25%, the COP continues to increase up to a certain point, beyond which it stabilizes. From Tg = 109°C for X_{NH_3} = 23% and Tg = 114°C for X_{NH_3} = 25%, the COP reaches 0.8984 and 1.285, respectively, before becoming almost constant. This phenomenon can be explained by the saturation of the heat exchange capacities in the generator, thus limiting the efficiency gains.

At higher pressures (low pressures) (1.4 and 1.7 bar), similar results are obtained. With an NH_3 concentration of 25% and a low pressure of 1.7 bar, the COP reaches a maximum of 0.910 at a generator temperature of 85°C. At these pressures, the COP seems to be more sensitive to variations in generator temperature, although it eventually stabilizes beyond a certain threshold, thus confirming the trend observed at lower pressure. Furthermore, the opposite effect is observed when observing the influence of the evaporator temperature on the COP. An increase in the evaporator temperature leads to a progressive decrease in the COP, which is attributable to the reduction of the thermal gradient necessary for the absorption process. It is also noted that lower pressures reduce the efficiency of the system, which highlights the importance of maintaining adequate pressure to optimize the cycle.

The performance shows that the maximum COP value is reached with an NH_3 concentration of 25% under a low pressure of 1 bar and an ambient temperature of 25°C, reaching 1.296. This indicates that the optimal conditions for the operation of these systems depend heavily on the NH_3 mass concentration, as well as the temperatures of the generator and evaporator.

In conclusion, this study demonstrates the importance of optimizing the NH_3 mass concentration (X_{NH_3}) in solar absorption refrigeration systems, taking into account the pressures and temperatures of the key components of the cycle. Proper management of these parameters not only maximizes the energy efficiency of the system but also ensures better utilization of solar heat sources. These results thus provide a solid basis for improving the performance of absorption machines and their integration into more sustainable cooling applications, particularly in regions with high solar irradiation where the demand for air conditioning is constantly increasing.

Volume 11, Issue 1, June 2025 - ISSN 2356-8569
http://dx.doi.org/10.21622/RESD.2025.11.1.1223

References

[1] A. Bermúdez and I. Padín, "Stochastic control with state constraints via the Fokker–Planck equation. Application to renewable energy plants with batteries," *Comptes Rendus. Mécanique*, vol. 351, no. S1, 2024, doi: 10.5802/crmeca.236.

[2] IEA, "The Future of Cooling – Analysis - IEA," Apr. 2018. [Online]. Available: https://www.iea.org/reports/the-future-of-cooling

[3] I. Sarbu and C. Sebarchievici, "Review of solar refrigeration and cooling systems," *Energy Build*, vol. 67, pp. 286–297, Dec. 2013, doi: 10.1016/j.enbuild.2013.08.022.

[4] R. Kühn, J. Römer, and F. Ziegler, "Comparison of ab- and adsorbents for low temperature heat driven sorption cooling machines," *International Journal of Refrigeration*, vol. 95, pp. 133–145, Nov. 2018, doi: 10.1016/j.ijrefrig.2018.07.019.

[5] H. Mohamed and A. Ben Brahim, "Modeling of the absorption phase of a cycle with solar absorption using the couple NH 3 –H 2 O for in-sight energy storage," *Int J Hydrogen Energy*, vol. 42, no. 13, pp. 8624–8630, Mar. 2017, doi: 10.1016/j.ijhydene.2016.06.183.

[6] M. A. Hammad and M. S. Audi, "Performance of a solar LiBr-water absorption refrigeration system," *Renew Energy*, vol. 2, no. 3, pp. 275–282, Jun. 1992, doi: 10.1016/0960-1481(92)90039-6.

[7] M. Wirtz, B. Stutz, H. T. Phan, and F. Boudehenn, "Combined generator for an NH3–H2O absorption chiller," *Int J Heat Mass Transf*, vol. 196, p. 123311, Nov. 2022, doi: 10.1016/j.ijheatmasstransfer.2022.123311.

[8] M. Benramdane, M. E. A. Ghernaout, and S. Abboudi, "Improved performance of solar installations absorption refrigeration," *Elsevier Ltd. and peer-reviewed by the Euro-Mediterranean Institute for Sustainable Development (EUMISD)*, 2014.

[9] Y. Liang, S. Li, X. Yue, and X. Zhang, "Analysis of NH3-H2O-LiBr absorption refrigeration integrated with an electrodialysis device," *Appl Therm Eng*, vol. 115, pp. 134–140, Mar. 2017, doi: 10.1016/j.applthermaleng.2016.10.202.

[10] M. Benramdane, M. Ghernaout, and S. Abboudi, "Effect of Pressure on Improving COP of a Refrigeration Installation Solar To Absorption," *International Journal of Engineering Research & Technology*, pp. 3–7, 2014.

[11] V. Jain, A. Singhal, G. Sachdeva, and S. S. Kachhwaha, "Advanced exergy analysis and risk estimation of novel NH3-H2O and H2O-LiBr integrated vapor absorption refrigeration system," *Energy Convers Manag*, vol. 224, p. 113348, Nov. 2020, doi: 10.1016/j.enconman.2020.113348.

[12] J. Sieres and J. Fernández-Seara, "Evaluation of the column components size on the vapour enrichment and system performance in small power NH3–H2O absorption refrigeration machines," *International Journal of Refrigeration*, vol. 29, no. 4, pp. 579–588, Jun. 2006, doi: 10.1016/j.ijrefrig.2005.10.004.

[13] B. Kumar, I. Selvarasan, G. Annadurai, and S. Ramalingam, "Thermodynamic analysis of a single effect lithium bromide water absorption system using waste heat in sugar industry," *Thermal Science*, vol. 22, no. 1, 2018, doi: 10.2298/tsci151013285b.

[14] Hilali İsmail and SÖYLEMEZ M., "An Application of Engine Exhaust Gas Driven Cooling System in Automobile Air-Conditioning System," *Isi Bilimi Ve Teknigi Dergisi/ Journal of Thermal Science and Technology*, vol. 35, no. 1, 2015.

[15] J. D. Marcos, R. Lizarte, F. Varela, M. E. Palacios-Lorenzo, and A. M. Blanco-Marigorta, "A solar air-cooled high efficiency absorption system in dry hot climates: Reduction of water consumption and environmental impact," *Thermal Science*, vol. 22, no. 5, 2018, doi: 10.2298/TSCI171204218M.

[16] E. Yildirim and B. Yeşilata, "DÜŞÜK SICAKLIKTA ISI KAYNAĞI KULLANAN BİR ABSORBS İYONLU THERMOECONOMIC OPTIMIZATION OF AN ABSORPTION SYSTEM USING HEAT," *Journal of Thermal Science and Technology*, vol. 33, no. 2, 2013.

[17] R. Ramesh, S. N. Murugesan, C. Narendran, and R. Saravanan, "Experimental investigations on shell and helical coil solution heat exchanger in NH 3 -H 2 O vapour absorption refrigeration system (VAR)," *International Communications in Heat and Mass Transfer*, vol. 87, pp. 6–13, Oct. 2017, doi: 10.1016/j.icheatmasstransfer.2017.06.010.

[18] S. Wang, S. Li, M. Xu, Z. Jin, and C. Xu, "SIMULATION RESEARCH ON ABSORPTION REFRIGERATION SYSTEM BASED ON NH3-H2O-LiBr VAPOR-LIQUID EQUILIBRIUM CALCULATION MODEL," *Thermal Science*, vol. 26, no. 2, 2022, doi: 10.2298/TSCI210127201W.

[19] B. Kilic and O. Ipek, "THERMODYNAMIC ANALYSIS OF ABSORPTION COOLING SYSTEM WITH LiBr-Al2O3-WATER NANOFLUID USING SOLAR ENERGY," *Thermal Science*, vol. 26, no. 1, 2022, doi: 10.2298/TSCI200817340K.

[20] V. Kumar, B. Pandya, J. Patel, and V. Matawala, "Cut-off temperature evaluation and performance comparison from energetic and exergetic perspective for NH3-H2O absorption refrigeration system," *Thermal Science and Engineering Progress*, vol. 4, 2017, doi: 10.1016/j.tsep.2017.09.007.

[21] A. Altamirano, N. Le Pierrès, and B. Stutz, "Review of small-capacity single-stage continuous absorption systems operating on binary working fluids for cooling: Theoretical, experimental and commercial cycles," *International Journal of Refrigeration*, vol. 106, pp. 350–373, Oct. 2019, doi: 10.1016/j.ijrefrig.2019.06.033.

[22] B. Narváez-Romo, M. Chhay, E. W. Zavaleta-Aguilar, and J. R. Simões-Moreira, "A critical review of heat and mass transfer correlations for LiBr-H 2 O and NH 3 -H 2 O absorption refrigeration machines using falling liquid film technology," *Appl Therm Eng*, vol. 123, pp. 1079–1095, Aug. 2017, doi: 10.1016/j.applthermaleng.2017.05.092.

[23] P. Waghare and A. Sathyabhama, "Performance analysis of ammonia-based vapour absorption refrigeration system," *Mater Today Proc*, vol. 51, pp. 1503–1509, 2022, doi: 10.1016/j.matpr.2021.10.279.

[24] D. Ali and W. Ratismith, "A semicircular trough solar collector for air-conditioning system using a single effect NH3–H2O absorption chiller," *Energy*, vol. 215, p. 119073, Jan. 2021, doi: 10.1016/j.energy.2020.119073.

[25] A. Aliane, S. Abboudi, C. Seladji, and B. Guendouz, "An illustrated review on solar absorption cooling experimental studies," *Renewable and Sustainable Energy Reviews*, vol. 65, pp. 443–458, Nov. 2016, doi: 10.1016/j.rser.2016.07.012.

[26] A. GHRICI, "Contribution à l'optimisation de l'efficacité énergétique des systèmes frigorifiques à Adsorption solaires," *Univ-tlemcen.dz*, 2023, doi: http://dspace.univ-tlemcen.dz/handle/112/20176.

[27] M. Benramdane, S. Abboudi, and S. Sevenans, "Contribution to Improving the Performance Coefficient of a Solar Absorption Refrigeration System," *international journal of research and reviews in applied sciences*, vol. 21, no. 2, 2014.

[28] A.-E. ALIANE, "Utilisation de l'énergie solaire thermique pour la production du froid," *Univ-tlemcen.dz*, 2019, doi: http://dspace.univ-tlemcen.dz/handle/112/14085.

[29] G. A. Florides, S. A. Kalogirou, S. A. Tassou, and L. C. Wrobel, "Modelling, simulation and warming impact assessment of a domestic-size absorption solar cooling system," *Appl Therm Eng*, vol. 22, no. 12, pp. 1313–1325, Aug. 2002, doi: 10.1016/S1359-4311(02)00054-6.

[30] M. Benramdane, S. Abboudi, and M. Ghernaout, "Contribution to the Simulation and Parametric Analysis of the Operation of a Solar Concentration Thermal Installation," *International Journal of Heat and Technology*, vol. 37, pp. 446–456, Apr. 2019, doi: 10.18280/ijht.370210.

[31] A. Kumbhar, N. Gulhane, and S. Pandure, "Theoretical Analysis of Hybrid Chiller," *Energy Procedia*, vol. 109, pp. 487–496, Mar. 2017, doi: 10.1016/j.egypro.2017.03.082.

[32] F. Dione, A. Thiam, E. I. Cisse, D. Diouf, and A. S. Maiga, "Theoretical study of an NH3–H2O absorption chiller powered by a linear Fresnel system modelled by combining ray tracing and CFD," *Results in Engineering*, vol. 20, p. 101410, Dec. 2023, doi: 10.1016/j.rineng.2023.101410.

[33] A. Ramanathan and P. Gunasekaran, "Simulation of absorption refrigeration system for automobile application," *Thermal Science*, vol. 12, no. 3, pp. 5–13, 2008, doi: 10.2298/TSCI0803005R.

[34] S. Akam, Z. Ouchiha, N. Said, and B. Bellal, "Expérimentation d'une Boucle à Absorption NH 3 -H 2 O," 1999. [Online]. Available: https://www.cder.dz/vlib/revue/nspeciauxpdf/jnv_4.pdf

[35] S. Kherris, M. Makhlouf, and A. Asnoun, "SARM: Simulation of Absorption Refrigeration Machine," *Journal of Renewable Energies*, vol. 11, no. 4, Dec. 2008, doi: 10.54966/jreen.v11i4.108.

[36] B. Narváez-Romo, M. Chhay, E. W. Zavaleta-Aguilar, and J. R. Simões-Moreira, "A critical review of heat and mass transfer correlations for LiBr-H 2 O and NH 3 -H 2 O absorption refrigeration machines using falling liquid film technology," *Appl Therm Eng*, vol. 123, pp. 1079–1095, Aug. 2017, doi: 10.1016/j.applthermaleng.2017.05.092.

[37] Y. Hang, M. Qu, and F. Zhao, "Economical and environmental assessment of an optimized solar cooling system for a medium-sized benchmark office building in Los Angeles, California," *Renew Energy*, vol. 36, no. 2, pp. 648–658, Feb. 2011, doi: 10.1016/j.renene.2010.08.005.

[38] "Programming with MATLAB 2016," 2016. [Online]. Available: https:// books.google .com .eg/ books ? hl =en & lr = & id = 2 e b U D A A A Q B A J & o i = f n d & p g = P A 1 & o t s = N B 7 6 v r D K t a & sig = X u B h 6 n 1iM R 2 6 x MyE_tsyZRfb Thg&redir_esc=y#v=onepage&q&f=false

[39] A. Allouhi, T. Kousksou, A. Jamil, T. El Rhafiki, Y. Mourad, and Y. Zeraouli, "Economic and environmental assessment of solar air-conditioning systems in Morocco," Renewable and Sustainable Energy Reviews, vol. 50, pp. 770–781, Oct. 2015, doi: 10.1016/j.rser.2015.05.044.

[40] Photovoltaic-software.com, "TRANSOL," 2017. [Online]. Available: https://photovoltaic-software.com/solar-thermal-softwares/professional-solar-thermal-softwares/transol

[41] R. Porumb, B. Porumb, and M. Balan, "Numerical Investigation on Solar Absorption Chiller with LiBr-H 2 O Operating Conditions and Performances," Energy Procedia, vol. 112, pp. 108–117, Mar. 2017, doi: 10.1016/j.egypro.2017.03.1071.

[42] "EES: Engineering Equation Solver | F-Chart Software : Engineering Software." [Online]. Available: https://fchartsoftware.com/ees/

[43] K. Wang, O. Abdelaziz, P. Kisari, and E. A. Vineyard, "State-of-the-art review on crystallization control technologies for water/LiBr absorption heat pumps," International Journal of Refrigeration, vol. 34, no. 6, pp. 1325–1337, Sep. 2011, doi: 10.1016/j.ijrefrig.2011.04.006.

[44] W. Wu, B. Wang, W. Shi, and X. Li, "An overview of ammonia-based absorption chillers and heat pumps," Renewable and Sustainable Energy Reviews, vol. 31, pp. 681–707, Mar. 2014, doi: 10.1016/j.rser.2013.12.021.

[45] R. Al-Rbaihat, H. Alahmer, A. Alahmer, Y. Altork, A. Al-Manea, and K. Y. E. Awwad, "Energy and exergy analysis of a subfreezing evaporator environment ammonia-water absorption refrigeration cycle: Machine learning and parametric optimization," International Journal of Refrigeration, vol. 154, pp. 182–204, Oct. 2023, doi: 10.1016/j.ijrefrig.2023.07.010.

[46] M. M. A. Khan, N. I. Ibrahim, R. Saidur, I. M. Mahbubul, and F. A. Al-Sulaiman, "Performance assessment of a solar powered ammonia–water absorption refrigeration system with storage units," Energy Convers Manag, vol. 126, pp. 316–328, Oct. 2016, doi: 10.1016/j.enconman.2016.08.004.

[47] W. Wu, W. Shi, J. Wang, B. Wang, and X. Li, "Experimental investigation on NH3–H2O compression-assisted absorption heat pump (CAHP) for low temperature heating under lower driving sources," Appl Energy, vol. 176, pp. 258–271, Aug. 2016, doi: 10.1016/j.apenergy.2016.04.115.